

---

# A modified kneed biped real robot based on parametric excitation principle

Yoshihisa Banno<sup>1</sup>, Kouichi Taji<sup>1</sup>, Yuji Harata<sup>2</sup>, Kyohei Seta<sup>1</sup>

<sup>1</sup>Department of Mechanical Science and Engineering, Graduate School of Engineering, Nagoya University, Furo, Chikusa, Nagoya, 464-8603, Japan

<sup>2</sup>Division of Mechanical Systems and Applied Mechanics, Faculty of Engineering, Hiroshima University, 1-4-1, Kagamiyama, Higashi-Hiroshima, 739-8527, Japan

## Email address:

y\_banno@nuem.nagoya-u.ac.jp (Y. Banno), taji@nuem.nagoya-u.ac.jp (K. Taji), harata@hiroshima-u.ac.jp (Y. Harata),

k\_seta@nuem.nagoya-u.ac.jp (K. Seta)

## To cite this article:

Yoshihisa Banno, Kouichi Taji, Yuji Harata, Kyohei Seta. A Modified Kneed Biped Real Robot Based on Parametric Excitation Principle.

*Automation, Control and Intelligent Systems*. Vol. 2, No. 5, 2014, pp. 93-99. doi: 10.11648/j.acis.20140205.14

---

**Abstract:** Parametric excitation walking is one of the bipedal gait generation methods on level ground. This method was first applied to a biped robot with telescopic legs and later to a kneed biped robot. An experimental robot with telescopic legs was also developed and it was verified that the robot could walk more than eight steps by the parametric excitation walking. Recently, we have developed an experimental kneed biped robot and have shown the robot can walk more than fifteen steps stably in inverse bending fashion. But the robot has a deficiency in that the robot does not have a ground sensor and the robot is controlled only in open-loop fashion. In this paper, we modify and improve the robot by using a ground sensor and shock absorbing material to enable to control in closed-loop fashion and hence, to improve the gait performance. The experiments are performed and the walking performance of the robot is investigated. The experimental results are compared with the numerical results, and the validity of the numerical simulation is verified.

**Keywords:** Parametric Excitation, Biped Robot, Passive Dynamic Walking, Experimental Robot, Walking Demonstration

---

## 1. Introduction

In recent two decades, the passive dynamic walking proposed in [1] has received much attention and has been studied extensively by many researchers. In passive dynamic walking, a robot walks down a slope stably and sustainably without any actuator, and passive dynamic walking has thought to be energy efficient. Inspired by passive dynamic walking, several walking method on level ground have been proposed, such as energy tracking control [2], virtual passive dynamic walking [3] and so on [4, 5].

The parametric excitation is another way of realizing passive dynamic-based walking on level ground. Parametric excitation is the principle to increase amplitude of vibration by changing a parameter periodically, and the principle is utilized to restore the energy lost by collision between a foot and the ground, and hence, sustainable walking is realized.

Reference [6] first applied the principle to the biped robot with telescopic legs which made the center of mass of swing leg up-and-down by pumping a leg, and showed that the

robot walked sustainably on level ground. Later in [7], bending and stretching a swing leg was shown to have the same effect of pumping a telescopic leg, and the parametric excitation walking for a kneed biped was proposed and was shown to walk sustainably on level ground. Reference [8] proposed the parametric excitation based inverse bending walking in which the knee of swing leg was bent in inverse direction to human movement. Reference [8] also showed that inverse bending was more energy efficient than forward bending like human movement by numerical experiments.

An experimental robot based on parametric excitation principle with telescopic legs was developed in [9], and the robot could walk about five steps on level ground. The robot was improved in [10] by adding a counterweight, which enabled the robot walking more than eight steps. Recently, an experimental kneed biped robot based on parametric excitation principle has developed in [11]. The robot has actuated knee joints, and [11] has shown that the robot can walk more than fifteen steps stably in inverse bending fashion.

But there is a big difference between the developed robot in [11] and simulation model in that the robot does not have a sensor to detect heel strike. In parametric excitation walking, it is known [7, 8, 12] that walking performance strongly depends on a reference trajectory of a swing leg knee joint, and a reference trajectory is designed to start at heel strike. Hence, in our previous experiments [11], both knee joints were controlled only to track a simple periodic reference trajectory in an open-loop control fashion.

In this paper, we improve the kneed biped robot developed in [11] by introducing a ground sensor and show new experimental results. The purpose of introducing a ground sensor is to detect the instance of heel strike, which makes the robot close to the simulation model and enables to control knee joints in a closed-loop way. Moreover, the ground sensor enables to change the start time of bending, which causes to the changes of walking speed and walking period for the same reference trajectory. This has already shown by simulation in [7, 8] and might improve stability and efficiency, but has not been verified by an experimental robot so far.

This paper is organized as follows. In Section 2, we introduce the model of a kneed biped robot dealt with in this paper and the control input for the robot to realize parametric excitation walking. In Section 3, we first introduce the experimental robot developed in [11], and then explain the improve points in detail. Experimental results are shown in section 4. Finally in Section 5, we conclude this paper.

## 2. Parametric Excitation Walking for a Kneed Biped Robot

Fig. 1 illustrates a biped robot model based on which we have developed an experimental robot. The model has five point masses, and has semicircular feet whose centers are on each leg. Semicircular feet were shown to have the same effects of equivalent ankle torque, and to decrease energy dissipation at heel strike [13]. We assume that only knees are actuated.

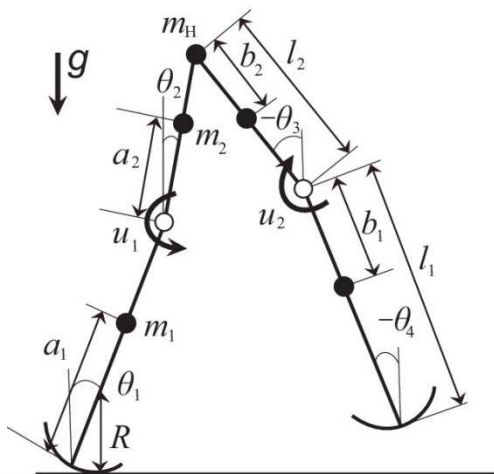


Fig. 1. Model of planar of kneed biped robot with semicircular feet.

The robot gait consists of the following two phases.

- Single support phase: A support leg rotates around the contact point between a semicircular foot and ground.
- Double support phase: This phase occurs instantaneously, and a support leg and the swing leg are exchanged after heel strike.

The dynamics of a robot during single support phase obeys the following equation of motion:

$$M(\theta)\ddot{\theta} + C(\theta, \dot{\theta})\dot{\theta} + g(\theta) = u, \quad (1)$$

where  $\theta = [\theta_1 \theta_2 \theta_3 \theta_4]^T$  is the generalized coordinate vector,  $M$  is the inertia matrix,  $C$  is the Coriolis force and the centrifugal force, and  $g$  is the gravity vector. The knee torque  $u$  is designed to realize parametric excitation walking.

The angular velocities  $\dot{\theta}^-$  and  $\dot{\theta}^+$ , immediately before and after the double support phase respectively, are related by the impact equation

$$\dot{\theta}^+ = J(\theta)\dot{\theta}^-, \quad (2)$$

where  $J$  is the translation matrix. The detail and the derivations of (1) and (2) are described in [14].

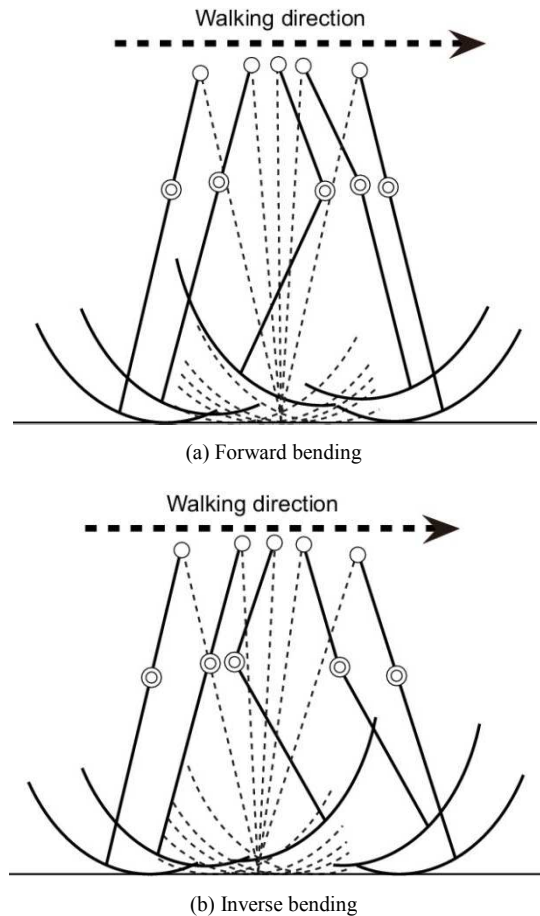


Fig. 2. Forward and inverse bending walking

In parametric excitation walking, the up-and-down motion of the center of mass by bending and stretching the swing leg knee restores mechanical energy lost at heel strike. Hence, it

is important to control the relative angle of the swing leg knee exactly according to the given relative knee angle. Because the control input  $u$  completely tracking the given relative knee angle was made by a partial feedback linearization method [7], it is sufficient to determine the appropriately designed the reference trajectory  $h(t)$  of the relative angle  $\theta_3 - \theta_4$  of the swing leg knee. To design the control input  $u$  according to the trajectory  $h(t)$  is also described in [14]. We note that, in the developed experimental robot, the knee joints are controlled by servomotors according to the given relative knee angle.

Reference [9] proposed the inverse bending walking in which a knee was bent in inverse direction to human movement. Stick diagrams of the forward bending and the inverse bending are shown in Fig. 2. In Fig. 2, the solid line represents a swing leg and the dashed line represents a support leg. The inverse bending walking was shown to restore larger energy than forward bending for the same reference trajectory in [9]. Because of this, we will compare the experimental results of the developed real robot with those of simulation results in the inverse bending walking only.

### 3. The Developed Kneed Biped Robot and its Modifications

In this section, we first introduce the experimental robot originally developed in [11], and then explain the improve points in detail.

#### 3.1. The Experimental Robot Developed in [11]

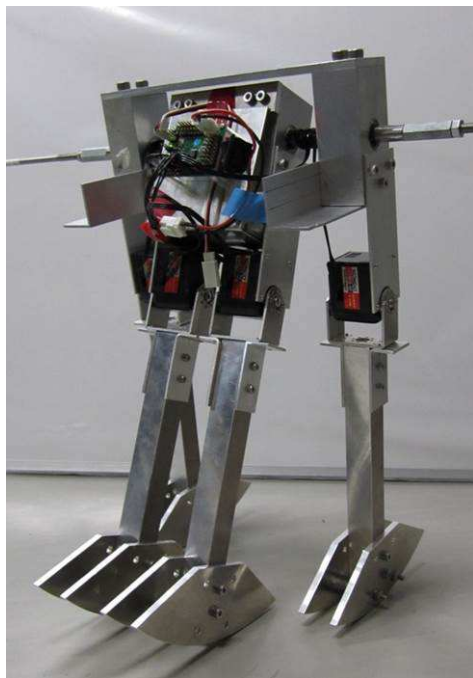


Fig. 3. Experimental robot

The experimental biped robot developed in [11] is shown in Fig. 3. The robot has four parallel legs. Each leg has a

semicircular foot and a knee joint with a servomotor. To restrict the robot movement in sagittal plane, the inside two legs and the outside two legs are synchronized, respectively. Upper legs are synchronized by structural constraint, of which the inside two upper legs and the outside two upper legs are connected by bars respectively, and lower legs are synchronized by control input with servo motors. A hip joint is free and has no actuators. Battery and controller are implemented on the inside two upper legs. To balance the inside two legs with the outside two legs, we put counterweights on the outside legs. A counterweight was shown to improve gait performance in [10]. Moreover, counterweights prevent the control board from damage when the robot falls down. The semicircular foot and counterweights of the robot are also shown in Fig. 3 and the physical parameters of the robot are shown in Table 1. Table 2 presents the control devices of the robot and the characteristics of the servomotor are shown in Table 3.

Table 1. Physical Parameters of the Robot

Upper leg length	0.10m
Lower leg length	0.22m
Foot radius	0.15m
Upper leg mass	0.10kg
Lower leg mass	0.35kg
Hip mass	1.25kg
Total mass	3.05kg

Table 2. Control devices (Manufactured by Kondo Kagaku Co.,Ltd.)

Devices	Product Name
Servo motor	KRS-4013HV
Control board	RCB-3HV
Battery	ROBO powercell

Table 3. The Performance of the servomotor

Maximum torque	2.65Nm
Maximum speed	83.3rpm
Weight	0.065kg

#### 3.2. Improved Points

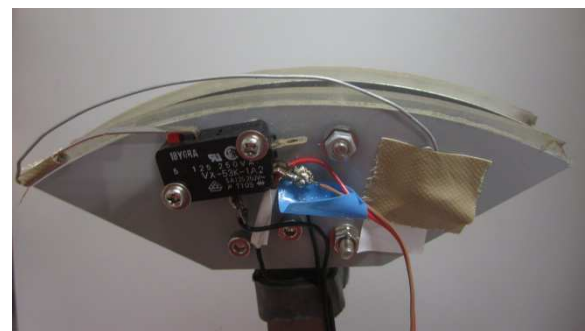


Fig. 4. Attached ground sensor and GEL tape

The improved points are two. One is to introduce a ground sensor. The experimental robot in [11] did not have a sensor to detect heel strike, and hence, both knee joints were controlled in an open-loop way. The ground sensor is made by micro switch (vx-53k-1A2, Omron Co. Ltd.) with a short

wire, and is attached on a semicircular foot. The attached ground sensor is shown in Fig. 4. In the figure, the wire is used to enlarge the region of landing detected by the micro switch.

We note that the function of the ground sensor is to send the signal to start bending another knee, rather than to detect the instant of heel strike. However, the experimental results in the later show that the instant of heel strike is detected almost exactly.

Another improved point is to attach the shock absorbing material on a semicircular foot. The parametric excitation walking proposed in [7, 8] has assumed that the semicircular foot of a support leg rolls on a ground without slipping. It has also assumed that the collision at heel strike is completely inelastic, that is, a swing leg lands without bouncing. Because the semicircular foot of the robot has been made by an aluminum board, we have required the specially equipped experimental road for demonstration experiments in [11]. The experimental road used in [11] consisted of a rubber sheet avoiding slipping and a shock absorbing material avoiding bouncing.

Instead of using the experimental road, we put the shock absorbing material, GEL Tape GT-5 (Taica co. [15]), on the arc of a semicircular foot. A GEL Tape is a very good material to resolve two issues simultaneously, slipping on a ground and bouncing at heel strike. The thickness of the GEL tape is only 3mm, and hence, we can ignore the change of a radius of semicircular foot. In Fig. 4, a GEL tape can be seen as translucent thin material on the arc.

Finally, we note that the use of GEL tape has practical meaning rather than theoretical one, in that it make the robot possible to walk on everywhere of flat and firm floor.

## 4. Experimental Results

In this section, we first present the overview of the experiment methodology and then we show the experimental results.

### 4.1. Overview of Experiment

To perform walking experiment, we first should design the reference trajectory of the relative angle,  $\theta_3 - \theta_4$ , for a swing leg knee. In the numerical simulation, the reference trajectory has been designed by sufficiently smooth curves, such as, the cubic sinusoid [7, 8] and quartic spline [12]. But the controller and the servo motor used in the developed robot can only control the certain angle to the target angle, the angle velocity between these two angles and the starting time of rotation by the signal of the attached grounding sensor. Hence, the designed reference trajectory is determined by five parameters: the starting time  $t_0$  of bending a swing leg from the heel strike, the relative angle  $A_0$  of a support leg knee, the maximum bending angle  $A_m$  of a swing leg knee, the duration time  $t_m$  of maintaining the maximum bending and the times  $t_b$  and  $t_s$  of bending time from  $A_0$  to  $A_m$  and stretching time from  $A_m$  to  $A_0$ , respectively.

In the demonstration experiments, the angle  $A_0$  is fixed as  $A_0 = 0.30\text{rad}$ , and the times  $t_b$ ,  $t_m$  and  $t_s$  are fixed as  $t_b = 0.21\text{s}$ ,  $t_m = 0.015\text{s}$  and  $t_s = 0.21\text{s}$ , respectively. We test for three maximum bending angles,  $A_m = 1.20, 1.35$  and  $1.50\text{rad}$ , and for each  $A_m$ , the starting time  $t_0$  is changed as  $t_0 = 0.075, 0.090$  and  $0.105\text{s}$ , that is, we test for nine reference trajectories. We note that the reason to introduce the positive support leg angle  $A_0 = 0.30\text{rad}$  is for a knee to avoid bending oppositely, and hence, the knee of the robot is always bending. The values of the parameters are set as the robot can walk, which are determined by trial and error in the experimental robot.

The lower, upper and relative knee angles during walking demonstration are measured by 3D motion capture system, OPTOTRAK Certus (Northern Digital Inc.). The motion capture system measures the positions of infrared-ray markers attached on the robot in 3D space by a camera and the markers invisible from the camera are not measured. Hence, we only measure the outside leg motion using four markers attached as shown in Fig. 5 with the 100Hz sampling rate.

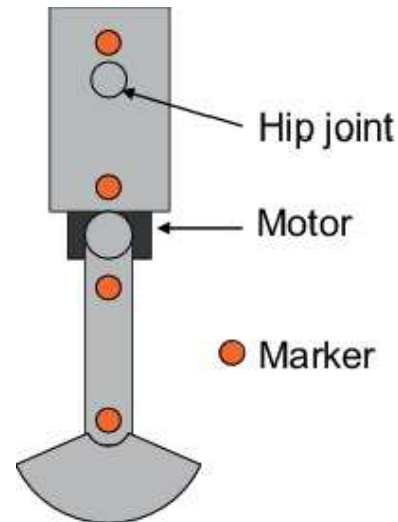


Fig. 5. Marker positions

To walk the robot, it is necessary to give an appropriate initial condition corresponding to a reference trajectory. This is very difficult in the simulations. But, in our demonstration experiment, this is resolved by the following simple method: the robot is held by hand until the gait becomes stable. In fact, the gait of the developed robot converges rapidly to steady gait within about seven or eight steps in our demonstration experiment, and hence the angles are measured after the first ten steps.

For the comparison purpose, we also perform numerical simulation. The reference trajectories of simulation are made with quartic spline to be close to the measured relative knee angles in demonstration experiment. We note that the reference trajectories used in simulation do not coincide with those in experiment by the limitation of the performance of a servo motor.

All experiments were performed on a wood board covered

by rubber sheets to avoid uneven road and make flat road.

#### 4.2. Experimental Results

For the nine reference trajectories explained above, we perform five walking trials for each case and measure walking data. The results of numerical simulations are

summarized in Table 4. In the table, we present the walking speed, the walking period and the step sizes for nine reference trajectories. All data are the average of measured data of the five trials for each reference trajectory. The results of numerical simulations are summarized in Table 5.

Table 4. The Results of Experiment

Maximum bending angle $A_m$ [rad]	Bending time $t_0$	Walking speed [m/s]	Waling period [s]	Step size [m]
1.20	0.075	0.259	0.559	0.145
	0.090	0.289	0.572	0.166
	0.105	0.294	0.578	0.170
1.35	0.075	0.331	0.559	0.185
	0.090	0.341	0.578	0.197
	0.105	0.342	0.586	0.200
1.50	0.075	0.370	0.568	0.209
	0.090	0.375	0.580	0.216
	0.105	0.378	0.588	0.222

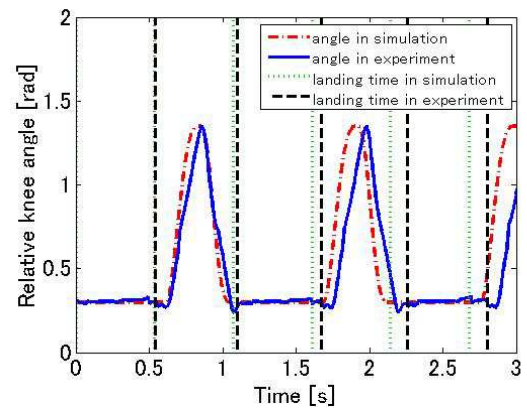
Table 5. The Results of Simulation

Maximum bending angle $A_m$ [rad]	Bending time $t_0$	Walking speed [m/s]	Waling period [s]	Step size [m]
1.20	0.075	0.331	0.524	0.173
	0.090	0.343	0.541	0.185
	0.105	0.350	0.554	0.194
1.35	0.075	0.354	0.536	0.190
	0.090	0.363	0.552	0.201
	0.105	0.369	0.566	0.209
1.50	0.075	0.375	0.546	0.205
	0.090	0.382	0.563	0.215
	0.105	0.386	0.578	0.223

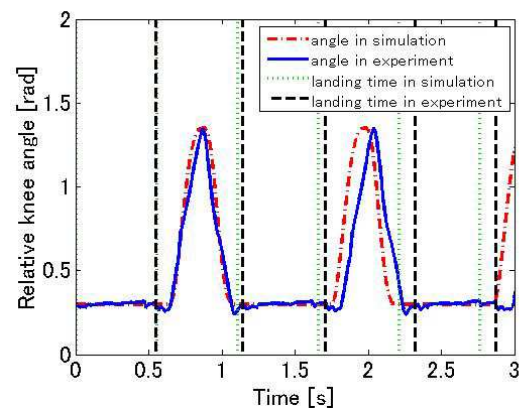
In all results, the robot walks more than twenty steps and the experimental results are the average of the measured five steps after than the first ten steps for each case. From the Table 4, we can observed that the walking speed, walking period and the step sizes of the experimental results are increasing as either the maximum bending angle is larger or the starting time of bending is later. These results are supported by the simulation results shown in Table 5. In particular, the differences of the results in the starting time  $t_0 = 0.075s$  and those of  $t_0 = 0.090s$  are larger than the differences between the results of  $t_0 = 0.090s$  and those of  $t_0 = 0.105s$ , for all three maximum bending angle in both experiments and simulations.

But there are differences between the experimental results and simulation results in that the walking speed and the step sizes of simulation results are larger than those of experiments, while the walking periods of both results are almost same. This is because some physical parameters, such as, inertia moments of legs are different between the simulations and experiments, and some friction in the hip joint and between foot and road does not taken in consideration in the simulation. To resolve the influences of these facts are one of the future research theme.

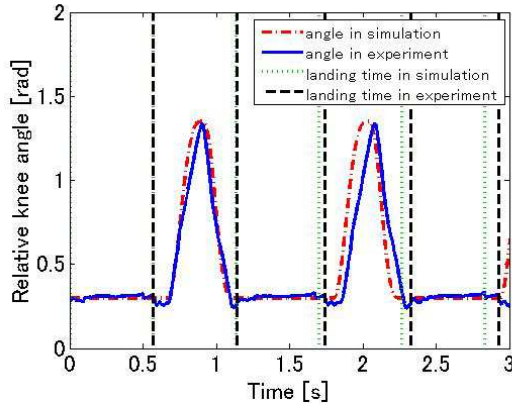
To see the results more in detail, we present the measured results of relative knee angles in Fig. 6, and the upper and the lower angles in Fig. 7 of the case of the maximum bending angle  $A_m = 1.35rad$ . In the Figs. 6 and 7, case (a) represents the results of starting time  $t_0 = 0.075s$ , case (b) represents  $t_0 = 0.090s$  and case (c) represents  $t_0 = 0.105s$ , and the blue solid lines denote the results of experiments and the red dotted lines denote those of simulation.



(a)  $A_m = 1.35rad$  and  $t_0 = 0.075s$

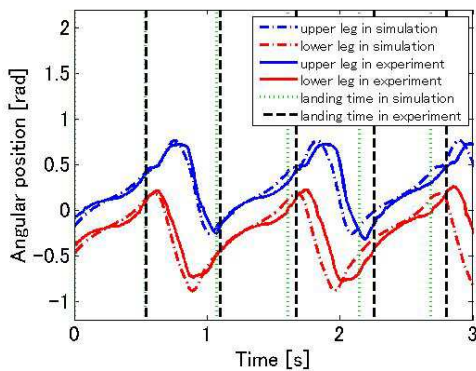


(b)  $A_m = 1.35rad$  and  $t_0 = 0.090s$

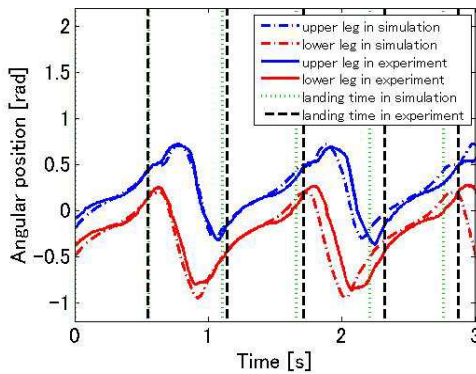


(c)  $A_m = 1.35\text{rad}$  and  $t_0 = 0.105\text{s}$

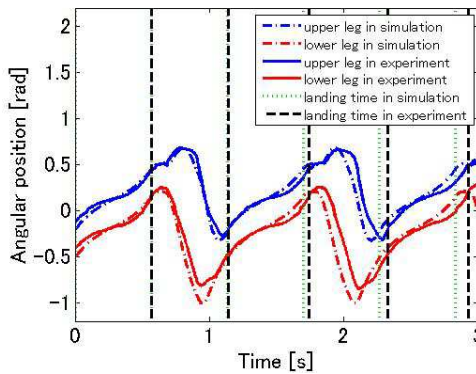
**Fig. 6.** Results of relative knee angles



(a)  $A_m = 1.35\text{rad}$  and  $t_0 = 0.075\text{s}$



(b)  $A_m = 1.35\text{rad}$  and  $t_0 = 0.090\text{s}$



(c)  $A_m = 1.35\text{rad}$  and  $t_0 = 0.105\text{s}$

**Fig. 7.** Results of angular positions

We also illustrate the instant of heel strike in the Figs. 6 and 7. In the figures, the instant of heel strike is denoted as follows: The black dotted lines denote the experimental results, and the green dotted lines denote simulation results. From Fig. 6, it is observed that the reference trajectories of the swing leg knee angle are followed exactly by servo motors. Furthermore, the starting time of bending coincides with the given starting time exactly for all three cases. This indicates that the attached grounding sensor can detect the instant of landing almost exactly. On the other hand, the results of experiment get delayed step by step because the period of experiment is longer than that of simulation. This is also observed in Fig. 7 in that the leg angles of experiments are very close to those of simulations, but after one or two steps, their differences are observed.

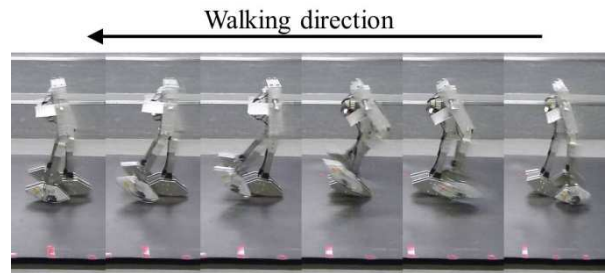


**Fig. 8.** Snapshots of walking demonstration

Finally, Fig. 8 represents the snapshots of the walking demonstration. Fig. 8 shows the serial photograph of one step of the case of  $A_m = 1.35\text{rad}$  and  $t_0 = 0.090\text{s}$ . Some movies of walking demonstrations are available at [16].

### 5. Conclusion

Parametric excitation-based inverse bending gait has been realized on level ground by modifying the previous biped real robot. The experimental results were compared with numerical results. These results can be summarized as follows:

- (1) The modification of the developed robot makes the gait generation based on parametric excitation principle on flat and firm ground without the experimental road consisted of a rubber sheet and a shock absorbing material.
- (2) Introducing the bending time by detecting heel strike improves walking speed and enlarges step size.
- (3) The experimental results were in good agreement with the numerical results, and the validity of the numerical was verified.

In the future, the parametric excitation-based walking on slope or uneven ground will be realized. In addition, reference trajectory where forward bending walking can be generated will be designed and the resultant walking compared with inverse bending walking.

We conclude the paper by giving remarks on the semicircular feet. Reference [13] has shown that a semicircular foot has two advantages, such as, a rolling effect corresponding to ankle torque and the reduction of

dissipation energy at heel strike, and hence, many robots with semicircular feet have been developed. But a robot with semicircular feet has a difficulty in that the robot cannot stand upright stance. To overcome this and simultaneously to realize energy efficiency, [17, 18] have proposed a robot with flat feet and ankle springs, [19] has proposed a robot with inerter in ankle joints. The primal purpose of the paper was to realize the parametric excitation walking with a real robot, and hence, we adopted the most simple foot configuration in the developed robot.

---

## References

- [1] T. McGeer, "Passive dynamic walking," *International Journal of Robotics Research*, vol. 9, no. 2, pp. 62-82, 1990.
- [2] A. Goswami, B. Espiau and A. Keramane, "Limit cycles in a passive compass gait biped and passivity-mimicking control laws," *Journal of Autonomous Robots*, vol. 4, no. 3, pp. 273-286, 1997.
- [3] F. Asano, M. Yamakita and K. Furuta, "Virtual passive dynamic walking and energy-based control laws," *Proceedings of the IEEE International Conference on Robotics and Systems*, Takamatu, Japan, vol. 2, pp. 1149-1154, 2000.
- [4] S. Collins, A. Ruina, R. Tedrake and M. Wisse, "Efficient bipedal robots based on passive-dynamic walkers," *Science*, vol. 307, pp.1082-1085, 2005.
- [5] E. Dertien, "Dynamic walking with dribbel," *IEEE Robotics and Automation Magazine*, vol. 13, no. 3, pp. 118-122, 2006.
- [6] F. Asano, Z. W. Luo and S. Hyon, "Parametric excitation mechanisms for dynamic bipedal walking," *Proceedings of the IEEE International Conference on Robotics and Automation*, pp. 611-617, 2005.
- [7] Y. Harata, F. Asano, Z. W. Luo, K. Taji and Y. Uno, "Biped gait generation based on parametric excitation by knee-joint actuation," *Robotica*, vol. 27, no. 7, pp. 1063-1073, 2009.
- [8] Y. Harata, F. Asano, K. Taji and Y. Uno, "Parametric excitation-based inverse bending gait generation," *Robotica*, vol. 29, no. 6, pp. 831-841, 2011.
- [9] F. Asano, T. Hayashi, Z. W. Luo, S. Hirano and A. Kato, "Parametric excitation approaches to efficient bipedal walking," *Proceedings of the IEEE/RSJ International Conference on Intelligent Robotics and Systems*, pp. 2210-2216, 2007.
- [10] T. Hayashi, F. Asano, Z.W. Luo, A. Nagano, K. Kaneko and A. Kato, "Experimental study of a parametric excited dynamic bipedal walker with counterweights," *Proceedings of the IEEE/RSJ International Conference on Intelligent Robots and Systems*, pp. 81-86, 2009.
- [11] Y. Banno, Y. Harata, K. Taji and Y. Uno, "Development and experiment of a kneed biped walking robot based on parametric excitation principle," *Proceedings of the 2011 IEEE/RSJ International Conference on Intelligent Robots and Systems*, pp. 2735-2740, 2011.
- [12] K. Taji, Y. Banno and Y. Harata, "An optimizing method for a reference trajectory of parametric excitation walking," *Robotica*, vol. 29, no. 4, pp. 585-593, 2011.
- [13] F. Asano and Z.W. Luo, "Efficient dynamic bipedal walking using effects of semicircular feet," *Robotica*, vol. 29, no. 3, pp. 3512-365, 2011.
- [14] Y. Harata, Y. Banno and K. Taji, "Parametric excitation based bipedal walking: control method and optimization," *Numerical Algebra, Control and Optimization*, vol. 1, no. 1, pp. 171-190, 2011.
- [15] <http://www.taica.co.jp/gel-english/>
- [16] <http://www.uno.nuem.nagoya-u.ac.jp/~taji/index-e.html>
- [17] T. Narukawa, K. Yokoyama and M. Takahashi, "Numerical and Experimental Studies of Planar Passive Biped Walker with Flat Feet and Ankle Springs," *Journal of System Design and Dynamics*, vol. 4, no. 6, pp. 848-856, 2010.
- [18] M. Wisse, D. G. E. Hobbelen, R. J. J. Rotteveel, S. I. Anderson and G. J. Zeglin, "Ankle springs instead of arc-shaped feet for passive dynamic walkers," *Proceedings of IEEE-RAS International Conference on Humanoid Robots*, pp. 110-116, 2006.
- [19] Y. Hanazawa and M. Yamakita, "High-Efficient Biped Walking Based on Flat-Footed Passive Dynamic Walking with Mechanical Impedance at Ankles," *Journal of Robotics and Mechatronics*, vol. 24, no. 3, pp. 498-506, 2012.